Persistent CH···π Interactions in Mefenamic Acid Complexes with Cyclic and Acyclic Amines

ARTICLE *in* CRYSTAL GROWTH & DESIGN · JUNE 2010

Impact Factor: 4.89 · DOI: 10.1021/cg100518b

5 AUTHORS, INCLUDING:

Marina S Fonari
Institute of Applied Physics Academy of Scie…
149 PUBLICATIONS **738** CITATIONS

SEE PROFILE

Eduard V. Ganin
Odessa State Environmental University
197 PUBLICATIONS **622** CITATIONS

SEE PROFILE

DOI: 10.1021/cg100518b

CRYSTAL GROWTH & DESIGN Article

2010, Vol. 10
3647–3656

Persistent CH···π Interactions in Mefenamic Acid Complexes with Cyclic and Acyclic Amines

Marina S. Fonari,*[,†] Eduard V. Ganin,[‡] Anna V. Vologzhanina,[#] Mikhail Yu. Antipin,[#] and Victor Ch. Kravtsov[†]

[†]*Institute of Applied Physics, Academy of Sciences of Moldova, Academiei Street, 5 MD-2028 Chişinău, R. Moldova,* [‡]*Odessa State Environmental University, Lvovskaya Street, 15, 65016, Odessa, Ukraine, and* [#]*A. N. Nesmeyanov Institute of Organoelement Compounds, Russian Academy of Sciences, 28 Vavilov St., B-334, 119991, Moscow, Russia*

Received April 19, 2010; Revised Manuscript Received May 28, 2010

ABSTRACT: Interaction of mefenamic acid [2-(2,3-dimethylphenyl)aminobenzoic acid, maH] with piperazine (ppz), 1,4,7,10-tetraazacyclododecane (cyclen), *meso*-5,7,7,12,12,14-hexamethyl-1,4,8,11-tetraazacyclotetradecane (teta), and tris-(hydroxymethyl)aminomethane (tris) resulted in crystalline proton-transfer complexes of the compositions $(ppzH_2)(ma)_2 \cdot 4H_2O$ **1**, $(cyclenH_2)(ma)_2 \cdot 2H_2O$ **2**, $(tetaH_2)(ma)_2 \cdot 2H_2O$ **3**, and $(trisH)(ma) \cdot H_2O$ **4**. Immediate cation−anion hydrogen bonds and those mediated by water molecules are the prime driving forces for the maH and amine assembly. Persistent CH···π interactions involving the aromatic rings were found to play an important role in the formation of final structures. All complexes reveal the pronounced segregation of hydrophilic and hydrophobic regions.

The active pharmaceutical ingredients (APIs) are most conveniently developed and delivered as solid dosage forms that contain a single crystalline form of an API due to the inherent stability of crystalline materials and the well-established impact of the crystallization processes on the purification and isolation of a chemical substance. However, there are often limitations in terms of solubility, stability, and bioavailability for the crystal form of a single organic molecule; thus the crystal form can be crucial to the performance of a dosage form.[1] Obviously, the variations in physicochemical properties can be achieved through structural variation, and pharmaceuticals may be manipulated, for example, by using different polymorphic forms, but the discovery of new polymorphs is often serendipitous and can be difficult to control.[2] Another possible way for modifying the physicochemical properties with the goal to improve pharmaceutical profile of drug is the creation of a multicomponent molecular complex (e.g., cocrystal or salt) without altering covalent bonding and therefore keeping the pharmacological behavior of the drug. Crystal engineering[3] has emerged into the pharmaceutical field with importance of its strategy in the design of multicomponent pharmaceutical solids.[4] The deliberate design of such organic solids, possessing controlled supramolecular structures, is generally based on conventional "strong" hydrogen bonds and robust, reproducible hydrogen bond motifs (synthons)[5] that occur with a high frequency in known crystal structures. Whereas stronger hydrogen bonds are ideal tools in this context, weaker interactions such as C−H···π, for example, are more problematic, although interactions involving aromatic systems are key processes in both chemical and biological recognition.[6] Moreover, in the structures rich with aromatic hydrocarbons the C−H···π interactions may dominate in molecular association, and packing thus playing an increasingly important role as a persistent structural motif in structure formation.[7] Therefore, it is believed that the C−H···π interactions are important in controlling the final structures of molecular assemblies, and it is a great challenge to make a full screen of various interactions changing from conventional strong hydrogen bonds to weak C−H···π interactions in the structure of relative molecular complexes.

Mefenamic acid [(2-(2,3-dimethylphenyl)aminobenzoic acid, maH] is a well-known representative of fenamates[8] showing a potent analgesic effect. Mefenamic acid is a nonsteroidal anti-inflammatory (NSAI), antipyretic, and analgesic agent that is used for the relief of postoperative and traumatic inflammation and analgesic treatment of rheumatoid arthritis, and antipyretic in acute respiratory tract infection.[9] Recently, it has been reported that maH is perspective as a therapeutic agent in Alzheimer's disease since it improves learning and memory impairment in an amyloid β peptide (Aβ1−42)-infused Alzheimer's disease rat model.[10] Low water solubility of maH limits its efficacy and therapeutic benefit as an API in the clinic; therefore, efforts have been done to enhance its solubility and dissolution rate.[11] The polymorphism of maH was studied for its effect on improvement physical properties. Similar to diclofenac, flufenamic, and tolfenamic acids that crystallize in three, two, and five polymorphic forms, respectively,[12] two crystalline polymorphic forms, stable Form I (CSD refcode XYANAC) and metastable Form II, were found for maH.[13] Since prodrugs are known to enhance numerous desirable qualities of pharmaceuticals and temporarily mask the acidic group to suppress gastrointestinal injury, the different esterified mefenamates were studied and approved as possible prodrugs.[14] Salts are usually considered as another alternative for drug delivery.[15] Sodium, manganese(II), cobalt(II), nickel(II), copper(II), and zinc(II) mefenamates were recently explored with the aim to solve the formulation and dissolution problems of maH.[16] On the other hand, the structural information for maH complexes with organic cocrystal partners is restricted by three salts with alkanolamines, *n*-propanol-, diethanol-, and triethanolamine (CSD refcodes NASBEP, NASBIT, NASBOZ, no fractional

*To whom correspondence should be addressed. E-mail: fonari.xray@phys.asm.md; kravtsov.xray@phys.asm.md; fax: +373 22 72 58 87; tel: +373 22 73 81 54.

Published on Web 06/08/2010

coordinates are available),[17] and an inclusion complex with cyclodextrin (CD).[18] As indicated by authors,[17] binary compounds of maH with alkanolamines represent the proton-transfer complexes sustained by the charge-assisted hydrogen bonds. Hydrophobic and hydrophilic regions exist in the crystal of each complex.

The diverse bases are successfully exploited nowadays as suitable cocrystallization partners for fatty, oxy-, and aromatic acids.[19,20] The advantages of polyazamacrocycles as *N*-bases are numerous.[21] In the polyprotonated form they are soluble in water. The high positive charge density and potential hydrogen-bonding sites promote complex formation with biologically relevant anionic substrates. The well-elaborated synthetic methodology provides the ring size readily varied in the synthetic scheme. Moreover, incorporated in the ring or attached as pendant arms organic moieties can vary their charge density and lipophilicity. For example, the pharmaceutically acceptable smallest in size cyclic diamine, piperazine, acts both in neutral and cationic forms giving rise to cocrystal with paracetamol,[22] and salts with salicylic, ascorbic, camphoric, pamoic acids, diclofenac, and phenylbutazone.[23]

Our previous research has been focused on the synthesis of multicomponent crystalline solids involving as APIs sulfa drugs,[24] or pharmaceutical acids, *p*-aminobenzoic acid,[25] salicylic acid,[26] and crown ethers (CEs) or azacycles as cocrystallization partners with an emphasis on the modes of interaction of the components in the solid state. *p*-Aminobenzoic acid yielded the binary molecular complexes of the 2:1 ratio with 18-membered CEs, while the proton-transfer complexes with mixed *N*,O-containing CEs and azacycles were obtained both for *p*-aminobenzoic and salicylic acids. In view of the above, our further attempts were aimed to design a system wherein an addition of a cyclic amine molecule could improve hydrogen bonding with maH, which in turn could impart physicochemical properties. For this purpose, the gradually increased in size aza cycles depicted in Scheme 1 along with one acyclic amine (tris) have been used. Piperazine and tris are pharmaceutically approved with their meaningful occurrence in the Cambridge Structural Database (CSD) as good crystal partners for APIs.[27] Within the past decade, tetraazacycles cyclen (1,4,7,10-tetraazacyclododecane) and cyclam (1,4,8,11-tetraazacyclotetradecane, the parent azacycle for teta) have found many applications in medicine. The advantages of cyclen and cyclam are their low toxicity, low molecular weight, and amphiphilic solubility.[21] All of these properties are beneficial for their investigation as suitable crystal partners. In general, ΔpK_a of an acid and a base is used as a rule of thumb to estimate the proton transfer.[28] The difference of 3.6−6 orders of magnitude between the acid dissociation constants of the base ($pK_a = 5.68$ and 9.82 for ppz, 10.51 and 9.49 for cyclen, 12.60 and 10.40 for teta, and 8.06 for tris),[29] and the acid ($pK_a = 4.2$ for maH[9a]) should lead to proton transfer and serves as an indication of the preferable formation of salts. So, with a high degree of probability we could expect the presence of ionic moieties in each structure under discussion.

Herein we report the synthesis and crystal structures of four novel complexes of maH with cyclic amines, piperazine (ppz), 1,4,7,10-tetraazacyclododecane (cyclen), *meso*-5,7,7,12,12,14-hexamethyl-1,4,8,11-tetraazacyclotetradecane (teta), and acyclic tris(hydroxymethyl)aminomethane (tris) of the compositions $(ppzH_2)(ma)_2 \cdot 4H_2O$ **1**, $(cyclenH_2)(ma)_2 \cdot 2H_2O$ **2**, $(tetaH_2)(ma)_2 \cdot 2H_2O$ **3**, and $(trisH)(ma) \cdot H_2O$ **4**.

Scheme 1. Target Mefenamic Acid and Amine Molecules with the Numbering Scheme

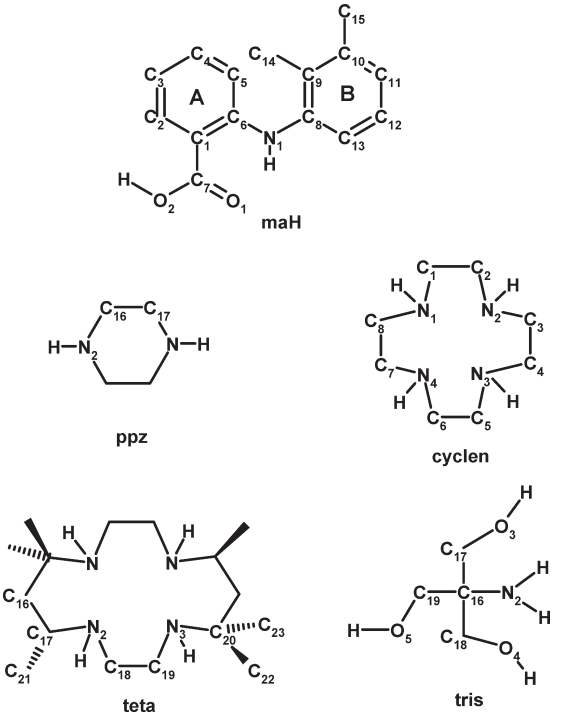

Experimental Section

General. All reagents (Scheme 1) were purchased from commercial sources and used as received. Solvents were obtained from commercial sources and distilled before use. Single crystals were obtained via slow evaporation of stoichiometric amounts of starting materials in an appropriate solvent. Compounds **1**−**4** were characterized by elemental analysis for C, H, and N in a Perkin-Elmer 240C device, X-ray powder diffraction (PXRD), and single crystal X-ray analysis.

$(ppzH_2)(ma)_2 \cdot 4H_2O$ 1. Piperazine hexahydrate (194 mg, 1 mmol) and maH (241 mg, 1 mmol) were dissolved upon boiling in methanol (25 mL). The solution was allowed to evaporate at room temperature when colorless transparent crystals appeared. mp 178−180 °C, found %: C 63.77; H 7.51; N 8.78%, required for $C_{34}H_{48}N_4O_8$ %: C 63.73; H 7.55; N 8.74.

$(cyclenH_2)(ma)_2 \cdot 2H_2O$ 2. 1,4,7,10-Tetraazacyclododecane (86 mg, 0.5 mmol) and maH (241 mg, 1 mmol) were dissolved upon boiling in a mixture of methanol, ethylacetate, and water (20 mL/50 mL/1 mL). The solution was allowed to evaporate at room temperature when colorless transparent needles appeared. mp 148−150 °C, found %: C 66.11%; H 7.84; N 12.19, required for $C_{38}H_{54}N_6O_6$ %: C 66.06; H 7.88; N 12.16.

$(tetaH_2)(ma)_2 \cdot 2H_2O$ 3. *meso*-5,7,7,12,12,14-Hexamethyl-1,4,8,11-tetraazacyclotetra-decane (142 mg, 0.5 mmol) and maH (241 mg, 1 mmol) were dissolved upon boiling in a mixture of methanol and ethylacetate (10 mL/30 mL). The solution was allowed to evaporate at room temperature when colorless transparent crystals appeared. mp 215−218 °C, found %: C 68.85; H 8.77; N 10.49, required for $C_{46}H_{70}N_6O_6$ %: C68.80; H 8.79; N 10.46.

$(trisH)(ma) \cdot H_2O$ 4. 2-Amino-2-(hydroxymethyl)propane-1, 3-diol (121 mg, 1 mmol) and maH (241 mg, 1 mmol) were dissolved in boiling water (15 mL). The solution was allowed to evaporate at room temperature when colorless transparent thin plates appeared. mp > 190 °C (melt. + dec.), found %: C 59.98; H 7.42; N 7.36, required for $C_{19}H_{28}N_2O_6$ %: C 59.93; H 7.45; N 7.39.

Single-Crystal X-ray Data Collection and Structure Determinations. The X-ray intensity data for **1**−**4** were recorded at 100 K on a Bruker-AXS SMART APEX/CCD diffractometer employing graphite monochromatized MoKα radiation ($\lambda = 0.71073$ Å) in ω scan mode. The structure solution and refinement proceeded similarly for all structures using SHELX-97 program package.[30] Direct

Table 1. Summary of the Crystal Data and Structure Refinement Parameters for 1−4

compound	1	2	3	4
formula	$C_{34}H_{48}N_4O_8$	$C_{38}H_{54}N_6O_6$	$C_{46}H_{70}N_6O_6$	$C_{19}H_{28}N_2O_6$
composition	$(C_4H_{12}N_2)(C_{15}H_{14}NO_2)_2\cdot 4H_2O$	$(C_8H_{22}N_4)(C_{15}H_{14}NO_2)_2\cdot 2H_2O$	$(C_{16}H_{38}N_4)(C_{15}H_{14}NO_2)_2\cdot 2H_2O$	$(C_4H_{12}NO_3)(C_{15}H_{14}NO_2)\cdot H_2O$
formula weight	640.76	690.87	803.08	380.43
crystal system	triclinic	monoclinic	triclinic	triclinic
space group	$P\bar{1}$	$C2/c$	$P\bar{1}$	$P\bar{1}$
a (Å)	6.9297(8)	32.809(4)	8.5654(14)	7.7773(16)
b (Å)	7.1741(8)	7.6594(10)	8.7181(14)	8.4070(17)
c (Å)	18.621(2)	29.684(4)	16.020(3)	15.127(3)
α (°)	85.995(2)	90.0	102.383(3)	90.642(4)
β (°)	83.245(2)	104.457(2)	91.415(3)	97.981(5)
γ (°)	65.812(2)	90.0	112.494(3)	97.970(4)
V (Å^3)	838.37(16)	7223.4(16)	1072.0(3)	969.6(3)
Z	1	8	1	2
D_c (Mg m^{-3})	1.269	1.271	1.244	1.303
μ (MoKα)/(mm^{-1})	0.091	0.087	0.083	0.097
F(000)	344	2976	436	408
reflections collected/unique	6659/3121 [R(int) = 0.0219]	26893/7094 [R(int) = 0.0563]	5612/3929 [R(int) = 0.0206]	7911/3797 [R(int) = 0.0284]
reflections with $I > 2\sigma(I)$	2565	5093	2886	2507
goodness-of-fit	1.008	1.008	0.999	0.963
R, wR [$I > 2\sigma(I)$]	0.0408, 0.1106	0.0545, 0.1236	0.0472, 0.1135	0.0361, 0.0705

methods yielded all non-hydrogen atoms. Hydrogen atoms bonded to nitrogen or oxygen atoms were localized in the difference Fourier map and refined freely with $U_{iso}(H) = 1.5_{eq}(O)$, $U_{iso}(H) = 1.2_{eq}(N)$. The remaining hydrogen atoms were placed in calculated positions and refined in "ride" mode. Structure graphics shown in the figures were created using the Mercury software package version 2.2.[31] Packing Index (PI) was calculated with the program PLATON.[32] Crystal data together with further details of the data collections and refinement are given in Table 1. CCDC reference numbers 759430−759433.

Results and Discussion

Commercially available maH, piperazine (ppz) hexahydrate, 1,4,7,10-tetraazacyclododecane (cyclen), *meso*-5,7,7,12,12,14-hexamethyl-1,4,8,11-tetraazacyclotetradecane (teta), and *tris*-(hydroxymethyl)methylamine (tris) were taken for cocrystallization. Crystalline products of the compositions $(ppzH_2)(ma)_2\cdot 4H_2O$ **1**, $(cyclenH_2)(ma)_2\cdot 2H_2O$ **2**, $(tetaH_2)(ma)_2\cdot 2H_2O$ **3**, and $(trisH)(ma)\cdot H_2O$ **4** were obtained in similar synthetic conditions in solution by direct mixing of maH with the basic component. The cycles gradually increase in size from 6 to 14 ring atoms, and contain two or four NH-amino groups capable of being protonated, contrary to one amino-group in tris. The purity of the synthesized compounds was confirmed by similarities between experimental and simulated X-ray powder diffraction patterns. The final complexes demonstrated the high stability within a long period of time. The melting point of all complexes falls between that of the partner and the drug substance, with no correlation with the melting points of initial bases (Table 2).[33] The variability in melting points for the series described herein may be attributed to the differences in structure, and primarily in the hydrogen bonding network. In **1**−**4** the acidic proton transfers from the carboxylic group of the maH molecule to the NH- or NH_2-group of the amine molecule give rise to the di- (**1**−**3**) or monocation (**4**). The crystallographic evidence for this proton transfer is the equalized C−O distances in the carboxylate group consistent with the carboxylate anion [bond distances C(7)−O(1) and C(7)−O(2) in Table 2, the most different values in the same COO^- group being 1.286(2) and 1.244(2) Å in **3**] and unbiased localization of the hydrogen atoms in close proximity to the nitrogen atoms in the *N*-basic cations, respectively. In all complexes the ma anion reveals an intramolecular N(1)−H···O(1) hydrogen bond of the $S_1^1(6)$ motif,[5] the N···O distance and N−H···O angle ranging within 2.624−2.675 Å and 132−143°, respectively (Table 3). The ma anion consists of the three planar fragments, the deprotonated carboxylic group, the phenyl ring **A** that carries it, and the xylyl ring **B** (Scheme 1). The conformation of the anion is defined by three torsion angles, O(1)−C(7)−C(1)−C(6), C(1)−C(6)−N(1)−C(8), and C(6)−N(1)−C(8)−C(9). These angles in **1**−**4** along with those in pure maH[13f] are given in Table 2. It can be clearly seen from Table 2 that the torsion angles C(1)−C(6)−N(1)−C(8) and C(6)−N(1)−C(8)−C(9) in **1**−**4** essentially vary. This fact indicates that the cocrystallization partner affects the observed conformation in the crystal structures.

Compound $(ppzH_2)(ma)_2\cdot 4H_2O$ **1** crystallizes in the triclinic space group $P\bar{1}$ (Figure 1). The piperazinium cation resides around an inversion center in chair conformation.

The seven-membered formula unit is stabilized by two charge-assisted $NH^+\cdots O(COO^-)$ hydrogen bonds using equatorial H-atoms, and two $NH\cdots O(H_2O)$ hydrogen bonds using axial H-atoms of azonia-groups, the cation···anion separation N(2)···O(1) of 2.713(2) Å (Table 3) being the shortest in the structure. There are no more direct cation−-anion interactions, and the two-membered O(1w)···O(2w) (2.726 Å) water clusters additionally link the charged entities inside the formula unit giving rise to two $R_4^4(13)$ graph sets. The second H-atom of each water molecule, being involved in the $OH(H_2O)\cdots O(COO^-)$ hydrogen bonds combines the formula units in the layer propagated parallel to the *ab* crystallographic plane (Figure 2).

The layer comprises the hydrophilic core and the hydrophobic outer surfaces. The internal hydrophilic region is formulated by the combination of the above-mentioned $R_4^4(13)$ motifs within the formula units, and alternating $R_4^6(12)$ and $R_6^6(16)$ motifs involving water molecules and carboxylic group of ma. Summarizing, six symmetry independent H-bonds are responsible for the stabilization of the hydrophilic area where all donors (two water molecules and one cyclic cation) are involved in single H-bonds, while the carboxylic oxygens act as multiple acceptors, taking part in three [O(1)] and two [O(2)] hydrogen-bonds, respectively. The parallel ma anions related by the shortest *a* and *b* translations demonstrate the edge-to-face arrangements of the **A** and **B**

Table 2. Selected Parameters of 1-4

parameter	**maH**[13f]	1	**2**		3	4
			a	**b**		
ma:base:H_2O ratio		2:1:4	2:1:2		2:1:2	1:1:1
melting point/°C	230−232	178−180	148−150		215−218	>190 (dec)
melting point base/ °C[a]		106	108−113		146−148	171−172
water environment		DDA, DDA	DDA, DD		DDA	DDA
O(1)−C(7) (Å)	1.232	1.278(2)	1.265(2)	1.262(2)	1.286(2)	1.270(2)
O(2)−C(7) (Å)	1.318	1.258(2)	1.258(2)	1.273(2)	1.244(2)	1.273(2)
C(6)−N(1)−C(8)−C(9) (°)	120.0	117.8(2)	79.3(3)	73.0(3)	160.4(2)	85.2(2)
C(1)−C(6)−N(1)−C(8) (°)	179.3	−172.2(1)	165.0(2)	−175.6(2)	145.1(2)	171.2(2)
O(1)−C(7)−C(1)−C(6) (°)	1.71	−7.6(2)	−7.0(3)	−6.3(3)	13.4(3)	6.8(2)
A/B angle (°)	62.4	60.6	73.4	75.3	53.5	78.4
CH (sp^2) ···π (Å)	3.59	3.41	3.91			3.44
	3.66	3.90				3.41
CH(sp^3) ···π (Å)	3.63	3.55	3.54		3.63	3.64
			3.83		3.67	
			3.99		3.74	
NH···π (Å)			3.47			
thickness of the layer (Å)	14.0	18.5	18.5		16.7	13.6
thickness of the hydrophobic region (Å)	14.0	13.9	12.2		14.1	11.4
area per one **ma**/($Å^2$)	45.4	45.4	56.8		69.0	64.8
packing index/(%)	68.2	69.1	69.8		70.9	69.4

[a] Melting point is given for anhydrous form.

Table 3. Hydrogen Bond Distances (Å) and Angles (°) for 1−4

D−H···A	*d*(D−H)	*d*(H···A)	*d*(D···A)	∠(DHA	symmetry transformation for acceptor
1					
N(1)−H(1N1)···O(1)	0.85(2)	2.00(2)	2.652(2)	133(2)	*x*, *y*, *z*
N(2)−H(1N2)···O(1)	0.98(2)	1.74(2)	2.713(2)	173(2)	*x*, *y*, *z*
N(2)−H(2N2)···O(2w)	0.91(1)	1.91(2)	2.808(2)	169(2)	2 − *x*, 1 − *y*, −*z*
O(1w)−H(1w1)···O(1)	0.87(2)	2.04(2)	2.851(2)	155(2)	1 + *x*, *y*, *z*
O(1w)−H(2w1)···O(2)	0.87(2)	1.96(2)	2.732(2)	147(2)	*x*, *y*, *z*
O(2w)−H(1w2)···O(1w)	0.90(2)	1.83(2)	2.726(2)	174(2)	*x*, *y*, *z*
O(2w)−H(2w2)···O(2)	0.92(2)	1.88(2)	2.802(2)	174(2)	3 − *x*, −*y*, −*z*
2					
N(1a)−H(1A)···O(1a)	0.88(2)	1.93(2)	2.641(2)	137(2)	*x*, *y*, *z*
N(1b)−H(1b)···O(1b)	0.88(2)	1.90(2)	2.625(2)	138(2)	*x*, *y*, *z*
N(1)−H(1N1)···O(2b)	0.96(2)	1.74(2)	2.697(2)	175(2)	*x*, *y*, *z*
N(1)−H(2N1)···N(4)	0.92(2)	2.37(2)	2.832(2)	111(2)	*x*, *y*, *z*
N(1)−H(2N1)···N(2)	0.92(2)	2.39(2)	2.874(2)	112(2)	*x*, *y*, *z*
N(1)−H(2N1)···O(1w)	0.92(2)	2.50(2)	3.021(2)	117(2)	*x*, *y*, *z*
N(3)−H(1N3)···O(1a)	1.01(2)	1.67(2)	2.664(2)	169(2)	*x*, *y*, *z*
N(3)−H(1N3)···O(2a)	1.01(2)	2.51(2)	3.192(2)	125(2)	*x*, *y*, *z*
N(3)−H(2N3)···N(2)	0.88(2)	2.35(2)	2.820(3)	114(2)	*x*, *y*, *z*
N(3)−H(2N3)···N(4)	0.88(2)	2.42(2)	2.885(2)	113(2)	*x*, *y*, *z*
N(4)−H(1N4)···O(2a)	0.92(2)	2.09(2)	2.925(2)	151(2)	1/2 − *x*, 1/2 + *y*, 1/2 − *z*
O(1w)−H(1w1)···O(2b)	0.87(3)	1.93(3)	2.806(2)	176(2)	1/2 − *x*, 3/2 − *y*, 1 − *z*
O(1w)−H(2w1)···O(1b)	0.88(3)	1.88(3)	2.752(2)	177(2)	*x*, *y*, *z*
O(2w)−H(1w2)···O(2a)	0.89(3)	1.95(2)	2.828(2)	170(3)	1/2 − *x*, 1/2 + *y*, 1/2 − *z*
O(2w)−H(2w2)···O(1w)	0.95(3)	1.94(3)	2.887(2)	175(3)	*x*, *y*, *z*
3					
N(1)−H(1N1)···O(1)	0.88(2)	1.91(2)	2.673(2)	144(2)	*x*, *y*, *z*
N(2)−H(1N2)···N(3)	0.90(2)	2.09(2)	2.829(2)	139(2)	1−*x*, −*y*, −*z*
N(2)−H(2N2)···O(1)	0.98(2)	1.81(2)	2.786(2)	171(2)	*x*, *y*, *z*
N(3)−H(1N3)···O(1w)	0.84(2)	2.34(2)	3.041(2)	141(2)	1 − *x*, −*y*, −*z*
O(1w)−H(1w1)···O(1)	0.87(3)	2.03(3)	2.873(2)	163(2)	*x*, *y*, *z*
O(1w)−H(2w1)···O(2)	0.87(3)	1.91(3)	2.777(2)	174(2)	1−*x*, 1−*y*, −*z*
4					
N(1)−H(1N1)···O(1)	0.84(2)	2.01(2)	2.676(2)	136(2)	*x*, *y*, *z*
N(2)−H(1N2)···O(3)	0.97(2)	1.88(2)	2.830(2)	167(2)	1−*x*, −*y*, 1−*z*
N(2)−H(2N2)···O(2)	0.95(2)	1.78(2)	2.723(2)	171(2)	*x*, *y*, *z*
N(2)−H(3N2)···O(5)	0.95(2)	1.83(2)	2.760(2)	169(2)	−*x*, −*y*, 1−*z*
O(1w)−H(1w)···O(2)	0.86(2)	1.93(2)	2.780(2)	174(2)	*x*, *y*, *z*
O(1w)−H(2w)···O(4)	0.89(2)	2.00(2)	2.859(2)	161(2)	1 − *x*, 1 − *y*, 1 − *z*
O(3)−H(3B)···O(1)	0.84	2.02	2.858(2)	176	1 − *x*, 1 − *y*, 1 − *z*
O(4)−H(4B)···O(1)	0.84	1.93	2.752(2)	167	*x*, *y*, *z*
O(5)−H(5B)···O(1w)	0.84	1.81	2.630(2)	166	1−*x*, −*y*, 1 − *z*

aromatic rings (Figure 2b, Table 2). The **A/B** dihedral angle of 60.6° between the interacting rings is equal to the **A/B** dihedral angle within the molecule. The layers meet by their hydrophobic surfaces and interactions across the layer boundary include the CH_3···π contacts[34] between the center-of-symmetry related xylyl rings (**B**) and directed outside the layer methyl groups, Figure 2c. The arrangement of ma anions both inside the layer and across the layer boundary closely

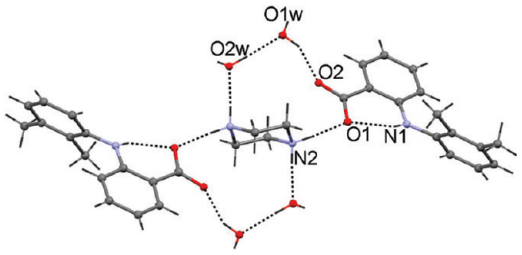

Figure 1. View of formula unit for **1** with the partial labeling scheme. Hydrogen bonds are shown by dashed lines.

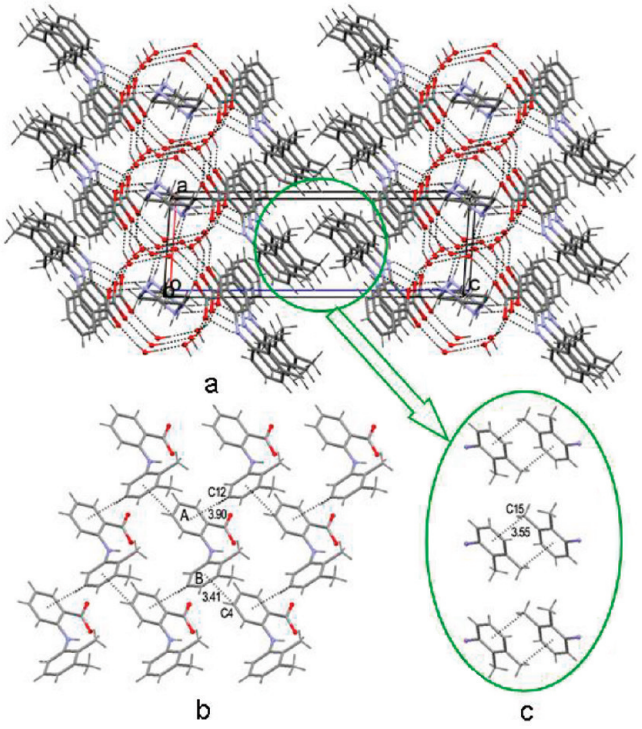

Figure 2. (a) Packing of two layers in **1**; (b) arrangement of ma anions in the slice parallel to the *ab* crystallographic plane. The edge-to-face CH(sp^2)$\cdots\pi$ interactions are shown by dotted lines; (c) the $CH_3\cdots\pi$ interactions of xylyl rings of ma anions in the interlayer region are shown by dashed lines.

resembles the crystal packing of the H-bonded centrosymmetric dimers of maH,[13f] which form similar layers with the hydrophilic carboxylic groups inside and two hydrophobic surfaces parallel to the crystallographic plane defined by the two shortest unit cell parameters. The only specific recognizable driving forces which hold the dimers within the layer are the edge-to-face **A/B** interactions between the related by translation maH molecules, C(4)−H$\cdots$Cg B(centroid B) = 3.59 Å, C(12)$\cdots$Cg B = 3.66 Å; the **A/B** dihedral angle equals 62.4°, resulting in exactly the same packing motif as shown in Figure 2b for **1**. It is also noteworthy that maH in the pure phase and ma in **1** occupy the same area of 45.4 $Å^2$ in the slice of parallel entities shown in Figure 2b. The conformations of maH and ma in **1** are also identical as is evident from Table 2. At the same time, the thickness of the layer given by the distance between the parallel planes defined by the most distal C(15) atoms is essentially different, being 14.0 Å in the structure of maH and 18.5 Å in **1**. Thus, the insertion of *N*-base between the ma entities affords the lateral expansion of the layer but preserves the intra- and interlayer CH$\cdots\pi$ interactions along with the relative arrangement of the anions in the structure.

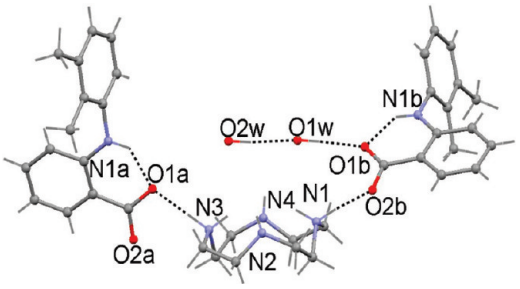

Figure 3. View of formula unit for **2** with the partial labeling scheme. Hydrogen bondings are shown by dashed lines.

Figure 3 depicts the five-membered complex (cyclenH_2)-(ma)$_2\cdot 2H_2O$ **2**, which crystallizes in the monoclinic space group *C*2/*c*. All the components, being the macrocyclic dication, two symmetry independent ma anions marked with the **a** and **b** trailers, and two water molecules, O(1w) and O(2w), occupy general positions. The anions **a** and **b** have similar conformations (Table 2). In the cyclic dication, each second nitrogen atom is additionally protonated, all four nitrogen atoms are perfectly coplanar (within 0.007 Å), and all *N*-bound hydrogen atoms display above this N_4 plane. The mode of protonation and the shape of the (cyclenH_2)$^{2+}$ moiety is identical to that found in its complex with *p*-aminobenzoic acid.[25b] The hydrogen atoms of the NH_2-groups are *endo*- and *exo*-oriented. The *endo*-oriented H-atoms participate in the bifurcated NH$\cdots$N intramolecular short contacts (Table 3). The *exo*-oriented H-atoms anchor the **a** and **b** anions via the charge-assisted $N^+\cdots O(COO^-)$ hydrogen bonds, N(1)$\cdots$O-(2b) 2.697(2) Å, and N(3)$\cdots$O(2a) 2.664(2) Å, being the shortest in **2** similar to **1** (Table 3). The formula unit is completed by the two-membered water cluster with the O(1w)$\cdots$O(2w) separation of 2.887(2) Å.

The neighboring complexes are associated in the tapes parallel to the *b* axis via the bridging carboxylic group of the anion **a** and the H-donor function of N(4) atom, the interaction being described by the $C_2^2(9)$ graph set. The water clusters additionally link the neighboring formula units into the tapes, mediating the **a** and **b** anions. The O(1w) water molecule uses one of its H-atoms for the cross-tape interactions giving rise to the layer spread parallel to the *bc* plane (Figure 4). These interactions generate the centrosymmetric heterotetramer, $R_4^4(12)$ that combines the two **b** anions and the two O(1w) water molecules.

Similar to **1**, the layer comprises the hydrophilic core and the hydrophobic outer surfaces and has the same thickness of 18.5 Å. However, the area occupied by one ma anion essentially increases and equals 56.8 $Å^2$, and the only one weak edge-to-face CH$\cdots\pi$ interaction with C(5a)$\cdots$Cg **B(b)** separation of 3.91 Å and the **A(a)**/**B(b)** dihedral angle of 76.8° preserves within the layer in **2**. It is a consequence of the insertion of the larger in size (cyclenH_2)$^{2+}$ cations which impose the increased separation between the pendant ma anions, while the more spongiose hydrophobic region of the layer facilitates the deeper interlayer interdigitation of the xylyl rings of the ma (Figure 4b, Table 2). Additionally, the structure reveals the NH$\cdots\pi$ interactions[35] of 3.47 Å, mediated by the cyclic NH-group and the unused π-acceptor function of ring **A** (anion **b**) Thus, the insertion of a larger cycle possessing an increased number of NH-binding sites does not enlarge the thickness of the layer but slides apart the neighboring ma anions.

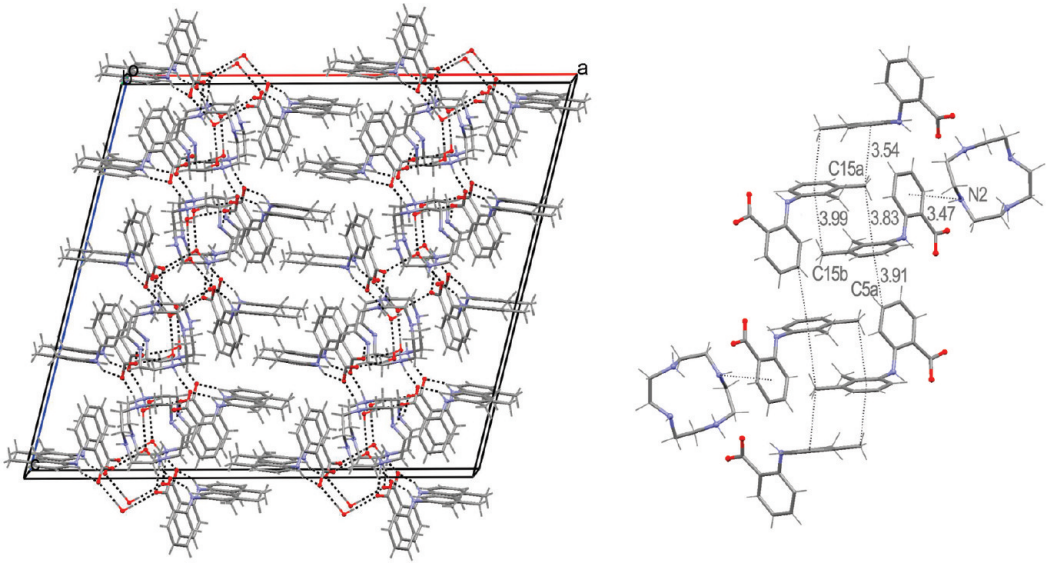

Figure 4. Crystal packing in **2**: (a) arrangement of two layers in the unit cell, (b) the CH$\cdots\pi$ and NH$\cdots\pi$ interactions involving aromatic rings are shown by dashed lines.

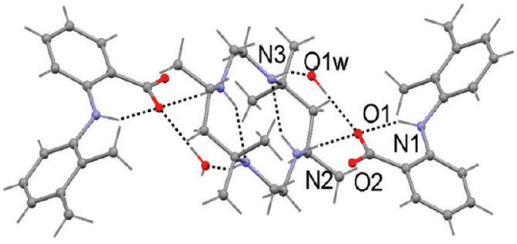

Figure 5. View of formula unit for **3** with the partial labeling scheme. Hydrogen bondings are shown by dashed lines.

Compound **3** of the composition $(tetaH_2)(ma)_2\cdot 2H_2O$ crystallizes in the triclinic space group $P\bar{1}$. The centrosymmetric formula unit is shown in Figure 5.

The mode of protonation of teta molecule is identical to that found in its complexes with 3- and 4-hydroxybenzoic acids, 3,5-dihydroxybenzoic and phenylphosphonic acids.[36] The conformation of the cation is fixed by the two N(2)−H$\cdots$N(3) hydrogen bonds. Complex **3** is stabilized by the combination of couples of $NH^+\cdots O(COO^-)$, $NH\cdots O(H_2O)$, and $OH(H_2O)\cdots O(COO^-)$ hydrogen bonds (Table 3). The neighboring complexes translated along the *b* direction are bound in the columns of the edge-fused $R_2^3(10)$ and $R_4^4(12)$ rings due to the bridging function of water molecule. The $R_4^4(12)$ graph set describes the centrosymmetric heterotetramer identical to that one found in **2** which combines two ma anions and two water molecules at O$\cdots$O distances of 2.776(2) and 2.871(2) Å, respectively (Figure 6). All possible hydrogen bonds are segregated inside the columns, which have the external hydrophobic surfaces.

The column size along the [001] direction defined as a separation between the parallel planes through the most distal C(15) atoms of the xylyl ring is 16.7 Å. The column size along the [100] direction defined by the planes through the C(3) atoms is 8.51 Å. The columns related by the translation along the *a* axis are connected by the CH$\cdots\pi$ interactions between the methyl group of the $(tetaH_2)^{2+}$ cation and ring **A** of the ma anion. To the opposite side of the **A** ring approaches the other

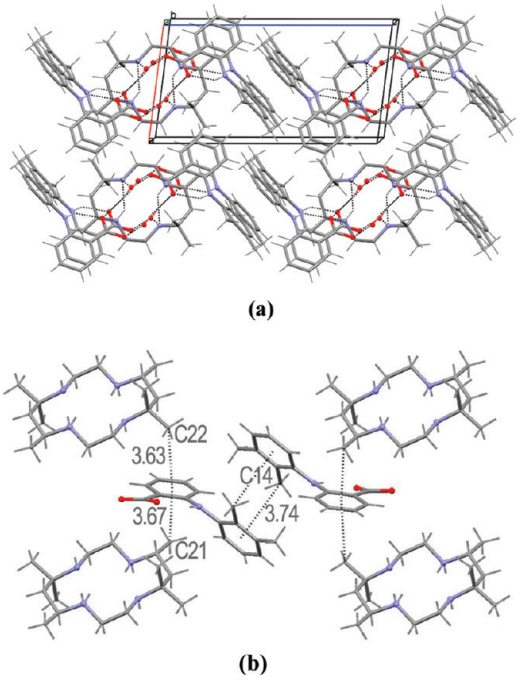

Figure 6. Crystal packing in **3** (a); the scheme of CH$\cdots\pi$ interactions shown by dashed lines (b).

methyl group of the $(tetaH_2)^{2+}$ showing the intracolumn CH$\cdots\pi$ interaction (Figure 6b). The methyl groups of the $(tetaH_2)^{2+}$ cation, intercalated into the slice of the parallel ma anions, substitute the edge-to-face interactions by the $CH_3\cdots\pi$ ones, which unite the columns in the layer similar to that found in **1**−**2**. The intervention of the methyl groups slides ma anions apart and increases up to 69.0 $Å^2$ the area occupied by one ma. The neighboring layers are stacked along the *c* axis via CH-$(sp^3)\cdots\pi$ interactions of 3.74 Å acting exactly in the same mode as in the pure maH and in **1**−**2**.

The proton-transfer complex $(trisH)(ma)\cdot H_2O$ **4** is the only one where the acyclic amine (Scheme 1) is used as a base.

Complex represents a monohydrate of the 1:1:1 stoichiometry, which crystallizes in the triclinic space group $P\bar{1}$. The formula unit is shown in Figure 7.

It is a solitary complex in this series where both oxygen atoms of the ma anion interact with the same cation in a chelate mode via the $NH(NH_3^+)\cdots O(COO^-)$ and $OH\cdots O(COO^-)$ hydrogen bonds giving rise to the $R_2^2(9)$ asymmetric ring. Three hydroxymethyl groups of *N*-base adopt around the amino-methyl bond a propeller-like conformation, close to the C_3 symmetry. The tripod geometry of the cation decorated by one NH_3^+ and three OH-groups facilitates its self-assembling in the chains running along the *a* axis which via bridging water molecules are further combined in the well-defined H-bonded layer developed parallel to the *ab* plane.

The similar self-organization of the $(trisH)^+$ cations in the chains is found in its deoxycholate,[37] while in the layer − in {2-[(2,6-dichlorophenyl)amino]phenylacetate.[38] The ma anions in **4** attached to the cationic layer via hydrogen bonds form its hydrophobic surfaces. The slice of the parallel ma anions reveals the same **B**/**A** edge-to-face interaction previously found in **1**−**2** and characterized by the $CH(sp^2)\cdots\pi$ and $CH(sp^3)\cdots\pi$ interactions (Figure 8b). Besides, cycle **B** is involved in the $CH(sp^3)\cdots\pi$ interaction of 3.41 Å with the methylene group of the $(trisH)^+$ cation. Each ma occupies an area of 64.8 $Å^2$. The layer in **4** is the thinnest among the studied complexes with a thickness of 13.6 Å between the planes defined by the most distal C(4) atom of ring **A**. This is explained by the rearrangement of the xylyl rings inside the layer due to its involvement in the intralayer $CH_3\cdots\pi$ interactions (Figure 8b).

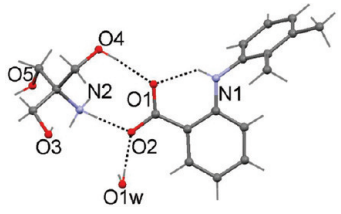

Figure 7. View of formula unit for **4** with the partial labeling scheme. Hydrogen bonds are shown by dashed lines.

The present study, our previous results,[25,26] and the literature data[20] unambiguously show that charge-assisted N−H···O hydrogen bonds are reliable and predictable interactions in the formation of organic complexes between aromatic carboxylic acids and cyclic amines in which nitrogen atom possesses sp^3-hybridization. These intermolecular interactions, being the shortest in the structure, determine the direct binding of *N*-base with aromatic carboxylate. A similar observation was made for the allied crystalline complexes with acyclic amines where the charge assisted N−H···O bonds were the driving forces for the aggregation of molecular components in the complex.[13] In all mefenamic acid−amine crystalline complexes known so far, the amine molecule inserts between the carboxylic groups of maH, disrupts the $R_2^2(8)$ carboxylic acid homomeric synthon, and replaces it by charge-assisted N−H···O hydrogen bonds. These strong H-bonds give the ability to control ma-amine assembly and represent an ideal tool for reproducing predesigned multicomponent crystals in this system.

The ability of organic crystals to form hydrated structures is very intriguing.[39,40] Structurally, hydrates of organic compounds have been categorized into two classes: isolated site hydrates and channel hydrates.[41] Because of their small size water molecules readily incorporate into crystal lattices and provide versatile hydrogen bonding patterns.[42] They can contribute to stabilization of crystal structures when there is an imbalance in the number of acceptors and donors[43] by forming a diverse arrangement of supramolecular heterosynthons. Our previous results for *p*-aminobenzoic acid complexes give such examples.[25] Referring to organic salts, the authors[27] based on the survey of CSD generalized the increasing hydrate formation with increasing charge on a single ion or with increasing number of carboxylate groups in a structure.[44] Recent studies represent the attempts to find correlations between the degree of hydration and thermal stability of the crystals.[45,46] Water molecules in **1**−**4** incorporate into the hydrophilic region of the crystals and feature different structural functions. The single water molecule point inclusion in the DDA (where D = H-donor, A = H-acceptor) environment is registered in **3** and **4**, while in **1**−**2** two crystallographically unique water molecules incorporate in the form

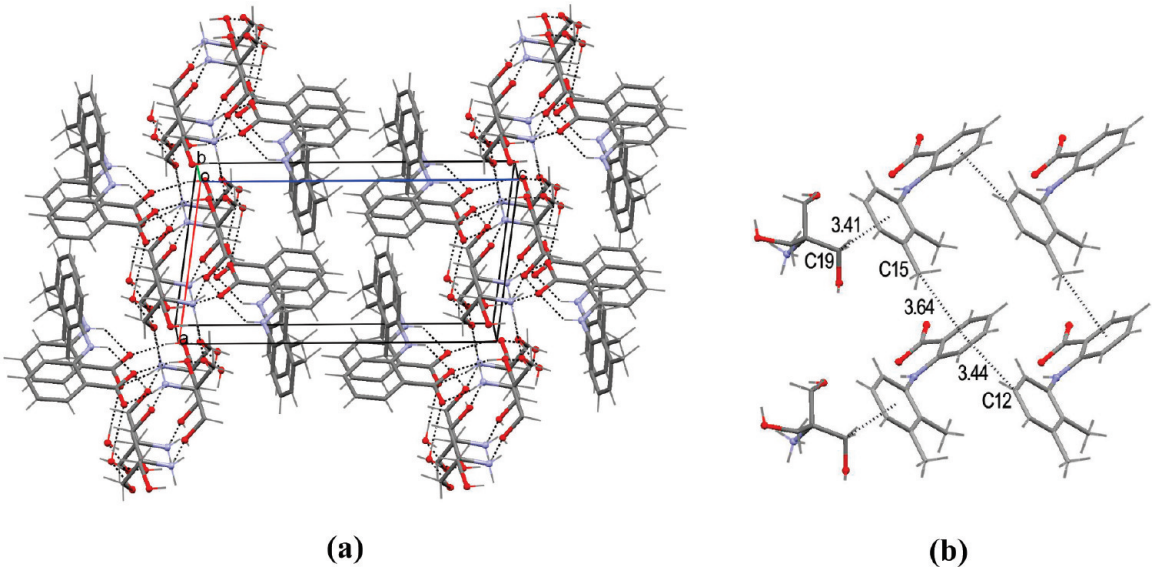

Figure 8. (a) Crystal packing in **4** shows the arrangement of two layers; (b) $CH\cdots\pi$ interactions involving aromatic rings are shown by dashed lines.

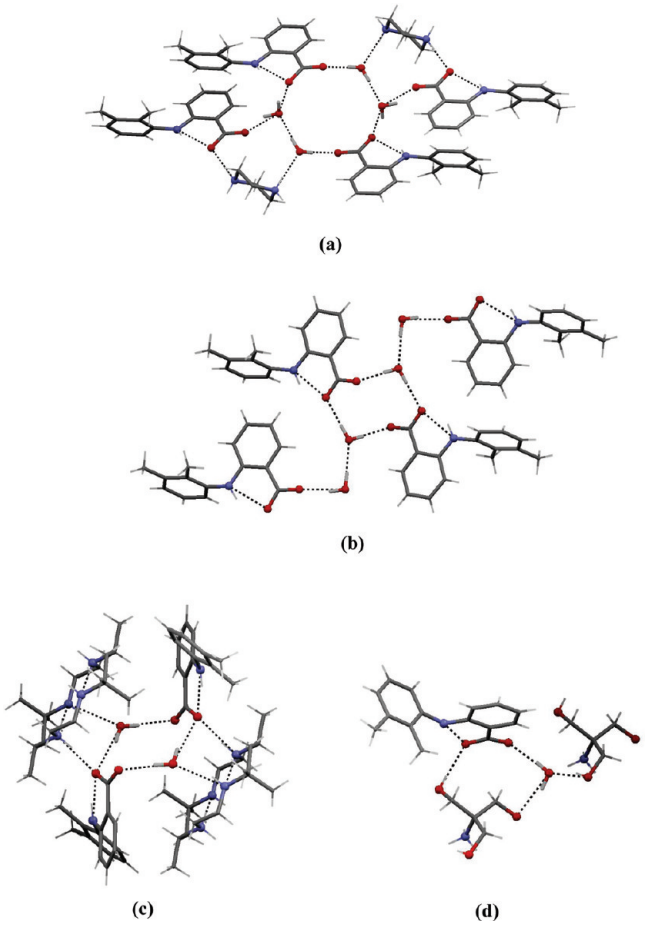

Figure 9. Water inclusion in **1** (a), **2** (b), **3** (c), and **4** (d).

of a two-membered cluster; in **1** both molecules exist in the same DDA environment, while in **2** exist in DDA and DD environments giving rise to the heteromeric clusters in the form of $R_6^4(16)$ (**1**), $R_4^4(12)$ (**2**, **3**), and $R_3^3(12)$ (**4**) H-bonded rings (Figure 9).

The contribution of CH$\cdots\pi$ intermolecular interactions to the overall system of interactions is the subject of intense debates nowadays.[47] The scientists agree that these interactions are very weak and being largely originated from the dispersion force they possess very weak directionality. For typical CHs in aliphatic and aromatic groups, the energy of one CH$\cdots\pi$ hydrogen bond is ca. 1.5−2.5 kcal mol^{-1}. Nevertheless, one of the most remarkable features of C−H$\cdots\pi$ interactions is that they work cooperatively, and this effect is most prominent in crystals.[48] For example, Kobayashi and Saigo[49] starting from the X-ray crystallographic structures for four less soluble organic salts sustained by the network of $NH_3^+\cdots O(COO^-)$ hydrogen bonds, using the periodic ab initio MO method presented computational evidence in favor of the cooperative effect of CH $\cdots\pi$ interactions in the crystals. The common feature of four complexes discussed herein is their layered structure in which the hydrophilic area is isolated within the layer. Whereas strong hydrogen bonds determine the ma-*N*-base assembly, the rather weak C−H$\cdots\pi$ intermolecular interactions predominate in the hydrophobic interlayer region and reported structures demonstrate their persistence (Table 2). The intra- and interlayer aromatic C−H$\cdots\pi$ interactions in the complexes iterate or resemble those in the pure phase of maH, although some of them are replaced by C−H$\cdots\pi$ or even N−H$\cdots\pi$ interactions with the base. These interactions determine the thickness of interlayer hydrophobic region formally evaluated as the distance between the parallel to layer planes through the outer for this region C(7) atoms of carboxylic groups. This parameter varies in a relatively short-range of 11.4−14.1 Å (Table 2). The major discrepancy in interlayer interactions and in such integrated parameters as thickness of the hydrophobic region compared with the pure phase of mefenamic acid was found for **4** which also differs from three other complexes by an ma/amine stoichiometry of 1:1. Only in **4** the acyclic amine, rich in donor-acceptor groups, and water molecules associate to form the well-defined H-bonded layer, which dictates the orientation of the attached to it ma anions. In the complexes with cyclic amines the formation of H-bonded layers or even columns occurs with involvement of carboxylic groups of ma; thus, the role of ma and competitive ability of weak C−H$\cdots\pi$ interactions in the tuning of overall packing pattern increase.

The ma anion reveals the conformational mobility indicated by the difference in the values of torsion angles around N(1)−C(8) and N(1)−C(6) bonds which comes up to 87.5° and 42.7°, respectively. At the same time, the dihedral angle between the aromatic rings, which influences the geometry of the C−H$\cdots\pi$ interactions, deviates in a relatively short range of 24.9°. The most effective crystal packing with the largest packing coefficient of 70.9% was found in complex **3** with the teta base enriched by the methyl groups.

Conclusions

Four novel crystalline complexes of mefenamic acid with *N*-bases, cyclic piperazine, 1,4,7,10-tetraazacyclododecane (cyclen), *meso*-5,7,7,12,12,14-hexamethyl-1,4,8,11-tetraazacyclotetradecane (teta), and acyclic tris(hydroxymethyl)aminomethane (tris) have been synthesized and studied. All complexes are formed due to the proton transfer from the carboxylic group of mefenamic acid to the amino group of *N*-base. The components are packed in the layers where the hydrophilic region within the layer is surrounded by two nonpolar surfaces formed by mefenamate anions. Notwithstanding a diverse hydrogen-bonding system including the most reliable charge-assisted hydrogen bonds between the mefenamate anions and cationic amines, the structures demonstrate persistent CH$\cdots\pi$ interactions both *within* and *across* the layers that include the aromatic moieties of the mefenamate anions. These interactions are closely comparable to those in the crystal structure of mefenamic acid itself, where the packing of the hydrogen-bonded dimers is directed by the well-defined edge-to-face interactions between the phenyl rings. Insertion of piperazine or cyclen into the mefenamic acid layers results in a lateral expansion within the layers but a minimal change in the interlayer interactions. Cocrystallization with teta demonstrates the competitive involvement of its own methyl groups into the $CH_3\cdots\pi$ interactions within the layer but the preservation of the interlayer packing motif. Cocrystallization with tris buries the xylyl rings of mefenamate anions within the layer thus decreasing the layer thickness and partly rearranging the interlayer hydrophobic interactions.

Acknowledgment. This work is supported by the Russian Foundation for Basic Research and the Academy of Sciences of R. Moldova (Project No. 08-03-90103-Mol-a/08.820.05.037RF)

Supporting Information Available: X-ray crystallographic information in CIF format. This information is available free of charge via the Internet at http://pubs.acs.org.

References

(1) (a) Huang, L. F.; Tong, W. Q. *Adv. Drug Delivery Rev*. **2004**, *56*, 321–334. (b) Singhal, D.; Curatolo, W. *Adv. Drug Delivery Rev*. **2004**, *56*, 335–347.

(2) (a) Bernstein, J. *Polymorphism in Molecular Crystals*; Oxford University Press: United Kingdom, 2003. (b) Dunitz, J. D.; Bernstein, J. *Acc. Chem. Res*. **1995**, *28* (4), 193–200. (c) Vishweshwar, P.; McMahon, J. A.; Oliveira, M.; Peterson, M. L.; Zaworotko, M. *J. Am. Chem. Soc*. **2005**, *127*, 16802–16803. (d) Hilfiker, R.; Blatter, F; von Raumer, M. In *Polymorphism in the Pharmaceutical Industry*; Hilfiker, R., Ed.; Wiley-VCH Verlag: Weinheim, 2006; Chapter 1, p 1.

(3) (a) Lehn, J. M. *Supramolecular Chemistry*; VCH: Weinheim, 1995; (b) Desiraju, G. R. *Crystal Engineering: the Design of Organic Solids*; Elsevier: Amsterdam, 1989; (c) B. Moulton, B.; Zaworotko, M. J. *Chem. Rev*. **2001**, *101*, 1629–1658.

(4) (a) Almarsson, O.; Zaworotko, M. J. *Chem. Commun*. **2004**, 1889–1896. (b) Vishweshwar, P.; McMahon, J.; Bis, J.; Zaworotko, M. J. *J. Pharm. Sci*. **2006**, *95*, 499–516. (c) Trask, A. V.; Motherwell, W. D. S.; Jones, W. *Cryst. Growth Des*. **2005**, *5*, 1013–1021. (d) Reddy, L. S.; Babu, N. J.; Nangia, A. *Chem. Commun*. **2006**, 1369–1371. (e) Basavoju, S.; Boström, D.; Velaga, S. P. *Cryst. Growth Des*. **2006**, *6*, 2699–2708.

(5) (a) Etter, M. *Acc. Chem. Res*. **1990**, *23*, 120–126. (b) Etter, M. C.; Frankenbach, G. A. *Chem. Mater*. **1989**, *1*, 10–12. (c) Desiraju, G. R. *Angew. Chem., Int. Ed. Engl*. **1995**, *34*, 2311–2327. (d) Desiraju, G. R. *Curr. Opin. Solid State Mater. Sci*. **1997**, *2*, 451–454.

(6) (a) Desiraju, G. R.; Steiner, T. *The Weak Hydrogen Bond in Structural Chemistry and Biology*; Oxford University Press: Oxford, 1999; (b) Meyer, E. A.; Castellano, R. K.; Diederich, F. *Angew. Chem., Int. Ed*. **2003**, *42*, 1210–1250.

(7) (a) Biradha, K.; Zaworotko, M. J. *J. Am. Chem. Soc*. **1998**, *120*, 6431–6432. (b) Lewis, G. R.; Dance, I. *J. Chem. Soc., Dalton Trans*. **2000**, 299–306. (c) Lewis, G. R.; Dance, I. *J. Chem. Soc., Dalton Trans*. **2000**, 3176–3185. (d) Scudder, M.; Dance, I. *J. Chem. Soc., Dalton Trans*. **1998**, 329–344.

(8) Mei, X.; August, A. T.; Wolf, C. *J. Org. Chem*. **2006**, *71*, 142–149.

(9) (a) Winder, C. V.; Wax, J.; Scotti, L.; Scherre, R. A.; Jones, E. M.; Short, F. W. *J. Pharmacol. Exp. Ther*. **1962**, *38*, 405–413. (b) Reynolds, J. E. F. *Martindale: The Extra Pharmacopoeia*, 31rd ed.; The Pharmaceutical Press: London, 1998; p 58; (c) Gungor, S.; Yildiz, A.; Ozsoy, Y.; Cevher, E.; Araman, A. *Farmaco* **2003**, *58*, 397–401.

(10) (a) Joo, Y.; Kim, H.-S.; Woo, R.-S.; Park, C. H.; Shin, Ki-Y.; Lee, J.-P.; Chang, K.-A.; Kim, S.; Suh, Y.-H. *Mol. Pharmacol*. **2006**, *69*, 76–84. (b) Asanuma, M.; Nishibayashi-Asanuma, S.; Miyazaki, I.; Kohno, M.; Ogawa, N. *J. Neurochem*. **2001**, *76*, 1895–1904.

(11) (a) Park, K. H.; Evans, J. M. B.; Myerson, A. S. *Cryst. Growth Des*. **2003**, *3*, 991–995. (b) Otsuka, M.; Kato, F.; Matsuda, Y. *Solid State Ionics* **2004**, *172*, 451–453. (c) Singh, A.; Lee, I. S.; Myerson, A. S. *Cryst. Growth Des*. **2009**, *9*, 1182–1185.

(12) (a) Castellari, C.; Ottani, S. *Acta Crystallogr*. **1997**, *C53*, 794–797. (b) Surov, A. O.; Terekhova, I. V.; Bauer−Brandl, A.; Perlovich, G. L. *Cryst. Growth Des*. **2009**, *9*, 3265–3272.

(13) (a) Adam, A.; Schrimpl, L.; Schmidt, P. C. *Drug. Dev. Ind. Pharm*. **2000**, *26*, 477–487. (b) Panchagnula, R.; Sundaramurthy, R.; Pillai, O.; Agrawal, S. *J. Pharm. Sci*. **2004**, *93*, 1019–1029. (c) Aguair, A. J.; Zelmer, J. E. *J. Pharm. Sci*. **1969**, *58*, 983–987. (d) Umeda, T.; Ohnishi, N.; Yokoyama, T.; Kuroda, T.; Kita, Y.; Kuroda, K.; Tatsumi, E.; Matsuda, Y. *Chem. Pharm. Bull*. **1985**, *33*, 2073–2078. (e) Lee, E. H.; Byrn, S. R.; Carvajal, T. M. *Pharm. Res*. **2006**, *23*, 2375–2380. (f) McConnell, J. F.; Company, F. Z. *Cryst. Struct. Commun*. **1976**, *5*, 861–864. (g) Romero, S.; Escalera, B.; Bustamante, P. *Int. J. Pharm*. **1999**, *178*, 193–202.

(14) (a) Jilani, J. A.; Najib, N. M.; Ghariabeh, S. H. *Acta Pharm. Hung*. **1997**, *67*, 99–104. (b) Tantishaiyakul, V.; Wiwattanawongsa, K.; Pinsuwan, S.; Kasiwong, S.; Phadoongsombut, N.; Kaewnopparat, S.; Kaewnopparat, N.; Rojanasakul, Y. *Pharm. Res*. **2002**, *19*, 1013–1018.

(15) (a) Aakeröy, Ch. B.; Fasulo, M. E.; Desper, J. *Mol. Pharmaceutics* **2007**, *4*, 317–322. (b) Berge, S. M.; Bighley, L. D.; Monkhouse, D. C. *J. Pharm. Sci*. **1977**, *66*, 1–19. (c) Agharkar, S.; Lindenbaum, S.; Higuchi, T. *J. Pharm. Sci*. **1976**, *65*, 747–749.

(16) (a) Bani−Jaber, A.; Hamdan, I.; Al-Khalidi, B. *Chem. Pharm. Bull*. **2007**, *55*, 1136–1140. (b) Kovala−Demertzi, D.; Hadjipavlou-Litina, D.; Staninska, M.; Primikiri, A.; Kotoglou, C.; Demertzis, M. A. *J. Enzyme Inhibition Med. Chem*. **2009**, *24*, 742–752. (c) Andrews, G. P.; Zhai, H.; Tipping, S.; Jones, D. S. *J. Pharm. Sci*. **2009**, *98*, 4545–4556. (d) Gupta, U.; Agashe, H. B.; Asthana, A; Jain, N. K. *Biomacromolecules* **2006**, *7* (3), 649–658.

(17) Fang, L.; Numajiri, S.; Kobayashi, D.; Ueda, H.; Nakayama, K.; Miyamae, H.; Morimoto, Y. *J. Pharm. Sci*. **2004**, *93*, 144–154.

(18) (a) Pop, M. M.; Goubitz, K.; Borodi, G.; Bogdan, M.; De Ridder, D. J. A.; Peschar, R.; Schenk, H. *Acta Crystallogr*. **2002**, *B58*, 1036–1043. (b) Hladon, T.; Pawlaczyk, J.; Szafran, B. *J. Incl. Phenom* **1999**, *35*, 497–506.

(19) Allen, F. N. *Acta Crystallogr*. **2002**, *B58*, 380–388.

(20) Skovsgaard, S.; Bond, A. D. *CrystEngComm* **2009**, *11*, 444–453.

(21) (a) Mertes, M. P.; Mertes, K. B. *Acc. Chem. Res*. **1990**, *23*, 413–418. (b) Liang, F.; Wan, S.; Li, Zh.; Xiong, X.; Yang, Li.; Zhou, X.; Wu, C. *Curr. Med. Chem*. **2006**, *13* (6), 711–727. (c) Delgado, R.; Felix, V.; Lima, L. M. P.; Price, D. W. *Dalton Trans*. **2007**, 2734–2745. (d) Chen, T.; Wang, X.; He, Y.; Zhang, C.; Wu, Z.; Liao, K.; Wang, J.; Guo, Z. *Inorg. Chem*. **2009**, *48*, 5801–5809.

(22) Oswald, I. D. H.; Allan, D. R.; McGregor, P. A.; Motherwell, W. D. S.; Parsons, S.; Pulham, C. R. *Acta Crystallogr*. **2002**, *B58*, 1057–1066.

(23) (a) Wang, C. K.-W.; Pan, Y.-J.; Jin, Z.-M. *Z. Kristallogr.- New Cryst. Struct* **2002**, *217*, 435–443. (b) Nomura, H.; Nakamachi, H.; Wada, Y. *Chem. Pharm. Bull*. **1982**, *30*, 1024–1029. (c) Zakaria, C. M.; Ferguson, G.; Lough, A. J.; Glidewell, C. *Acta Crystallogr*. **2003**, *B59*, 118–131. (d) Du, M.; Zhang, Z.−H.; Guo, W.; Fu, X.−J. *Cryst. Growth Des*. **2009**, *9* (4), 1655–1657. (e) Castellari, C.; Sabatino, P. *Acta Crystallogr*. **1996**, *C52*, 1708–1712. (f) Castellari, C.; Ottani, S. *Acta Crystallogr*. **1998**, *C54*, 415–417. (g) Singh, T. P.; Vijayan, M. *J. Chem. Soc., Perkin Trans*. **1977**, *2*, 693–699.

(24) (a) Fonari, M. S.; Ganin, E. V.; Tang, S.-W.; Wang, W.-J.; Simonov, Yu. A. *J. Mol. Struct*. **2007**, *826*, 89–95. (b) Fonari, M. S.; Ganin, E. V.; Simonov, Yu. A.; Wang, W.-J. *Acta Crystallogr*. **2006**, *E62*, o911–o913. (c) Simonov, Yu. A.; Fonari, M. S.; Bocelli, G.; Calestani, G.; Lipkowski, J.; Suwinska, K.; Ganin, E. V. *Supramol. Chem*. **1995**, *4*, 251–258.

(25) (a) Basok, S. S.; Bocelli, G.; Fonari, M. S.; Ganin, E. V.; Simonov, Yu. A. *Acta Crystallogr*. **2006**, *C62*, o50–o52. (b) Moulton, B.; Luisi, B. S.; Fonari, M. S.; Basok, S. S.; Ganin, E. V.; Kravtsov, V. Ch. *New J. Chem*. **2007**, *31*, 561–568.

(26) Fonari, M. S.; Kravtsov, V. Ch.; Simonov, Yu. A.; Basok, S. S.; Ganin, E. V. Supramolecular Architecture in the Co-Crystals of Azacrown Ethers with Salicylic Acid. Moldavian-Polish-Ukrainian Symposium on Supramolecular Chemistry, Chisinau, Moldova, October 10−12, **2005**, Abstracts, p 65.

(27) Haynes, D. A.; Jones, W.; Motherwell, W. D. S. *J. Pharm. Sci*. **2005**, *94*, 2111–2120.

(28) (a) Ratajczak, H.; Sobczyk, L. *J. Chem. Phys*. **1969**, *50*, 556–557. (b) Li, Z. J.; Abramov, Yu.; Bordner, J.; Leonard, J.; Medek, A.; Trask, A. V. *J. Am. Chem. Soc*. **2006**, *128*, 8199–8210.

(29) (a) Hetzer, H. B.; Robinson, R. A.; Bates, R. G. *J. Phys. Chem*. **1968**, *72*, 2081–2086. (b) Kodama, M.; Kimura, E. *J. Chem. Soc., Dalton Trans*. **1980**, 327–333. (c) Pesavento, M.; Profumo, A.; Soldi, T.; Fabbrizzi, L. *Inorg. Chem*. **1985**, *24*, 3873–3875. (d) El-Harakany, A. A.; Abdel Halima, F. M.; Barakat, A. O. *J. Electroanal. Chem*. **1984**, *162* (1−2), 285–305.

(30) Sheldrick, G. M. *Acta Crystallogr*. **2008**, *A64*, 112–122.

(31) Macrae, C. F.; Edgington, P. R.; McCabe, P.; Pidcock, E.; Shields, G. P.; Taylor, R.; Towler, M.; van de Streek, J. *J. Appl. Crystallogr*. **2006**, *39*, 453–457.

(32) Spek, A. L. *J. Appl. Crystallogr*. **2003**, *36*, 7–13.

(33) The successful attempts are reported to fine-tune melting points and aqueous solubility by incorporation of an API within a series of crystalline solids characterized by considerable structural consistency: (a) Aakeroy, Ch. B.; Forbes, S.; Desper, J. *J. Am. Chem. Soc*. **2009**, *131*, 17048–17049. (b) Stanton, M. K.; Bak, A. *Cryst. Growth Des*. **2008**, *8*, 3856–3862.

(34) (a) Re, S.; Nagase, S. *Chem. Commun*. **2004**, 658–659. (b) Nishio, M. *CrystEngComm* **2004**, *6* (27), 130–158.

(35) Braga, D.; Grepioni, F.; Todesco, E. *Organometallics* **1998**, *17*, 2669–2672.

(36) Gregson, R. M.; Glidewell, C.; Ferguson, G.; Lough, A. L. *Acta Crystallogr*. **2000**, *B56*, 39–57.

(37) (a) Tusvik, P. H.; Mostad, A.; Dalhus, B.; Rosenqvist, E. *Acta Crystallogr*. **1999**, *C55*, 1113–1115. (b) Ng, S. W. *Z. Kristallogr*. **1995**, *210*, 287–289.

(38) Castellari, C.; Ottani, S. *Acta Crystallogr*. **1997**, *C53*, 482–486.

(39) Infantes, L.; Fabian, L.; Motherwell, W. D. S. *CrystEngComm* **2007**, *9*, 65–71.

(40) Rodriguez-Spong, B.; Price, Ch.P.; Jayasankar, A.; Matzger, A. J.; Rodriguez-Hornedo, N. *Adv. Drug. Delivery Rev*. **2004**, *56*, 241–274.

(41) Morris, K. R. In *Polymorphism in Pharmaceutical Solids*; Brittain, H. G., Ed..; Marcel Dekker Inc.: New York, 1999, 125−181.
(42) Gillon, A. L.; Feeder, N.; Davey, R. J.; Storey, R. *Cryst. Growth Des.* **2003**, *3*, 663–673.
(43) Desiraju, R. G. *J. Chem. Soc., Chem. Commun.* **1991**, 426–428.
(44) Infantes, L.; Chisholm, J.; Motherwell, S. *CrystEngComm* **2003**, *5*, 480–486.
(45) Kiang, Y.-H.; Xu, W.; Stephens, P. W.; Ball, R. G.; Yasuda, N. *Cryst. Growth Des.* **2009**, *9*, 1833–1843.
(46) Clarke, H. D.; Arora, K. K.; Bass, H.; Kavuru, P.; Ong, T. T.; Pujari, T.; Wojtas, L.; Zaworotko, M. J. *Cryst. Growth Des.* **2010**, *10*, 2152–2167.
(47) (a) Tsuzuki, S.; Honda, K.; Uchimaru, T.; Mikami, M.; Fujii, A. *J. Phys. Chem. A* **2006**, *110*, 10163–10168. (b) Tsuzuki, S.; Fujii, A. *Phys. Chem. Chem. Phys.* **2008**, *10*, 2584–2594.
(48) (a) Nishio, M.; Umezawa, Y.; Honda, K.; Tsuboyama, S.; Suezawa, H. *CrystEngComm* **2009**, *11*, 1757–1788. (b) Bissantz, C.; Kuhn, B.; Stahl, M. *J. Med. Chem.* doi: 10.1021/jm100112j.
(49) Kobayashi, Y.; Saigo, K. *J. Am. Chem. Soc.* **2005**, *127*, 15054–15060.